Journal of Applied Polymer Science

Assessment of Ball Milling Methodology to Develop Polylactide-Bacterial Cellulose Nanocrystals Nanocomposites

Jesús Ambrosio-Martín,[1] Amparo Lopez-Rubio,[1] María José Fabra,[1] Giuliana Gorrasi,[2] Roberto Pantani,[2] Jose María Lagaron[1]

[1]Novel Materials and Nanotechnology Group, IATA, CSIC, Av. Agustín Escardino 7, 46980 Paterna (Valencia), Spain
[2]Department of Industrial Engineering, University of Salerno, Via Giovanni Paolo II 132, 84084 Fisciano Salerno, Italy
Correspondence to: J. M. Lagarón (E-mail: lagaron@iata.csic.es)

ABSTRACT: In this work, ball milling is evaluated as a methodology to develop polylactide (PLA)-bacterial cellulose nanocrystals (BCNC) nanocomposites. This technique, widely used for clay-based nanocomposites, is effective in breaking up to a very large extent the freeze-dried nanocellulose aggregates, giving raise to transparent films similar to the neat PLA films. Incorporation of the nanofiller through this methodology enhances the polymer crystallinity index. An increase in the onset degradation temperature and a significant reinforcing effect in terms of an increase in the storage modulus and in the tan delta peak are also observed. Improved barrier to oxygen at high relative humidity (80%) is also noticed, reaching the best performance at the lowest BCNC loading (0.5 wt %). These improvements are related to the relatively good nanocellulose dispersion and distribution attained for low loadings of the nanofiller. Thus, the ball milling methodology appears as a feasible processing methodology for developing PLA-BCNC nanocomposites. © 2014 Wiley Periodicals, Inc. J. Appl. Polym. Sci. **2015**, *132*, 41605.

KEYWORDS: biopolymers & renewable polymers; composites; films; nanoparticles; nanowires and nanocrystals; packaging

Received 4 August 2014; accepted 10 October 2014
DOI: 10.1002/app.41605

INTRODUCTION

The development of fully renewable biopolymer nanocomposites to replace synthetic polymers for different applications has been the subject of numerous studies during the last years. Nanocellulose [also referred to as cellulose nanocrystals (CNC) or cellulose nanowhiskers] represents one of the most interesting fillers for these applications due to its broad availability, low cost, and to the possibility of obtaining different morphological features depending on the cellulose source. In this sense, while CNC extracted from vegetal resources such as cotton or wood typically have a length of 100–300 nm and width of 5–20 nm,[1–3] those obtained from tunicin and bacterial cellulose (BCNC) may have several micrometres in length and a width of 5–50 nm.[4–6] CNC are usually obtained through hydrolysis with strong acids such as sulphuric acid or hydrochloric acid, which produce a preferential digestion of the amorphous domains of the material and cleavage of the nanofibril bundles.[7] One of the main difficulties associated with the use of unmodified CNC as reinforcing agents is their high hydrophilicity, which makes it difficult to disperse them in non-polar media. This is especially relevant when trying to implement the physical properties of biopolyesters using nanocellulose. Among the biopolyesters, polylactide (PLA) obtained from the fermentation of corn starch[8] is one of the most attractive materials due to its high transparency and ease of processability and thus has found commercial applications in food packaging and medicine. However, PLA also presents a number of drawbacks such as low thermal resistance, excessive brittleness, and relatively low barrier to oxygen and water vapor as compared to other packaging materials such as polyethylene terephthalate. The other great challenge when trying to develop PLA-based nanocomposites reinforced with CNC is to attain proper nanofiller dispersion through the use of industrial processing techniques, such as melt compounding methods, due to the above mentioned different nature between hydrophobic PLA and hydrophilic CNC. It has been observed that direct melt mixing of the freeze-dried nanocellulose with the polymer or biopolymer matrix provides materials with big nanocellulose agglomerates and thus insufficient physical properties.[9] Several strategies have been recently developed to improve nanocellulose dispersion in PLA matrices obtained through melt compounding, based on pre-incorporation of the nanofiller either in electrospun fibres[9] or in lactic acid oligomers.[10] Chemical modification of the nanofiller has also been investigated, and although improved adhesion with the PLA matrix was observed, good nanofiller dispersion was only obtained for low nanocellulose loadings.[11] Moreover, chemical

modification also resulted in decreased crystallinity and thermal stability of the nanofiller.[11] As an alternative, the potential of ball milling has been previously investigated to develop polymer nanocomposites where hydrophilic filler was introduced in hydrophobic matrix, attempting to overcome the lack of natural affinity between both components.[12] Ball milling is a high-energy grinding technique, able to induce several mechanochemical changes in the materials that occur at different rates. In addition to its use to develop clay-based nanocomposites, this technique has been previously used in the development of graphene-based nanocomposites as the high-energy milling induces platelet and graphite delamination, respectively, thus improving the final properties of the obtained materials.[13] Very recently, nanofibres of 50 nm diameter were obtained from waste jute fibres using high energy planetary ball milling,[14] thus suggesting that this high mechanical energy process could be effectively used for improving nanocrystals dispersion. To the best of our knowledge, this technique has not been used before to generate cellulose-based nanocomposites and; thus, the objective of the present work was to evaluate the potential of ball milling for the production of PLA-BCNC nanocomposites and to compare it with the existing strategies previously developed. PLA and freeze-dried BCNC were ground together using ball milling and the mixed material obtained was subsequently hot-pressed into films. The morphology, thermal properties, isothermal crystallization, mechanical properties, and oxygen barrier performance of the so-obtained nanocomposites were characterized.

EXPERIMENTAL

Materials

The semicrystalline poly(lactic acid) (PLA) used was a film extrusion grade with a number average molecular weight (M_n) of 130,000 g mol^{-1} and a weight average molecular weight (M_w) of 150,000 g mol^{-1} manufactured by NatureWorks. Prior to the ball milling process, the material was purified by dissolution in $CHCl_3$ and subsequent precipitation by drop-wise addition to an excess of methanol. The material, in this way, was transformed from pellet to powder form which is necessary for the ball milling process. Sulphuric acid 96 wt % and sodium hydroxide pellets were purchased from Panreac (Barcelona, Spain). The bacterial strain *Gluconacetobacter xylinus* was obtained from the Spanish type culture collection (CECT).

Preparation of Bacterial Cellulose Nanocrystals (BCNC)

Initially, bacterial cellulose mats were obtained using the bacterial strain *Gluconacetobacter xylinus* 7351 as described in previous works.[10,15] After that BCNC were obtained by acid hydrolysis using the optimized method reported by Martinez-Sanz and coworkers.[7] Full description of the synthesis of the BCNC can be found elsewhere.[10]

Preparation of Nanocomposites Through Ball Milling

Grinded BCNC and PLA powder were milled in the solid state in a Retsch (Germany) centrifugal ball mill (model PM100). The milling process was carried out in a cylindrical steel jar of 50 cm^3 with five steel balls of 10 mm of diameter. The rotation speed used was 650 rpm, and the milling time was fixed to 60 min. In these experimental conditions, four series of composites PLA-BCNC with 0.5, 1, 3, and 5 wt/wt % of BCNC were prepared. An additional PLA sample to be taken as a reference was also milled in absence of filler. The PLA-BCNC mixtures and the pure milled PLA were molded in a hot press (Carver Inc.) at 165°C forming 250 ± 50 μm thick films.

Optical Properties of the Films

The opacity of the films was measured by using a Konica Minolta CM-2500d X-Rite SP60 Series spectrophotometer following the ASTM E284 ("Terminology of Appearance"). The opacity was defined as ability of a thin film to hide a surface behind and in contact with it, expressed as the ratio of the reflectance factor (R_b) when the material is backed by a black surface to the reflectance factor (R_w) when it is backed by a white surface (usually having a reflectance factor of 0.89). The opacity (O) was calculated using the relationship: $O\ (\%) = (R_b/R_w) \times 100$

Differential Scanning Calorimetry (DSC)

The thermal properties and isothermal cold crystallization behavior of PLA and PLA-BCNC nanocomposite films obtained through ball milling were studied by DSC using a DTA Mettler Toledo (DSC 30) under nitrogen atmosphere. DSC experiments were carried out on typically 10–12 mg of dry material at a heating and cooling rate of 10°C min^{-1}. To ensure reliability of the data obtained, heat flow and temperature were calibrated with standard materials, indium, and zinc.

The degree of crystallinity (%) of PLA was estimated from the corrected enthalpy for biopolymer content in the final materials, using the ratio between the enthalpy of the studied material and the enthalpy of a perfect PLA crystal, that is, $\%X_c = (\Delta H_f - \Delta H_c)/\Delta H_f^o$; where ΔH_f is the enthalpy of fusion and ΔH_c the enthalpy of cold crystallization of the of the studied specimen. ΔH_f^o is the enthalpy of fusion of a totally crystalline material. The ΔH_f^o used for this equation was 93 J g^{-1} for PLA.[16]

In addition, isothermal crystallization kinetics study was performed as follow. The samples were heated from room temperature to 180 at 75°C min^{-1} and held for 10 min to erase the thermal history. Then, they were cooled rapidly at 100°C min^{-1}, to the desired crystallization temperatures (in this case 105, 110, and 115°C), ensuring that the crystallization process do no start in the cooling step. After that, the temperature was held for about 2 h, until the crystallization process was completed, and finally heated at 10°C min^{-1} to 180°C again to get the melting temperature.

Thermogravimetric Analysis (TGA)

Thermogravimetric (TG) curves were recorded using a thermobalance Mettler TC-10. The samples were heated from 25 to 800°C at a heating rate of 10°C min^{-1} both under air flow and under nitrogen atmosphere. The weight loss was recorded as function of temperature.

Dynamic Mechanical Analysis (DMA)

Mechanical properties were evaluated using a DMA TAQ800. Measurements were conducted at the constant frequency (1 Hz) and amplitude (5 μm). The temperature was varied between −30 and 140°C at 3°C min^{-1}.

Oxygen Transmission Rate

The oxygen permeability coefficient was derived from oxygen transmission rate (OTR) measurements recorded using an

Table I. Opacity Values of Films with Different BCNC Contents

BCNC content (%)	Apparent opacity
0	16.4 ± 0.2
0.5	16.3 ± 0.1
1	16.0 ± 0.9
3	17.3 ± 0.1
5	19.5 ± 0.2

Oxtran 100 equipment (Modern Control Inc., Minneapolis, MN). Experiments were carried out at 24°C and at 80% relative humidity (RH) conditions. Relative humidity was generated by a built-in gas bubbler and was checked with a hygrometer placed at the exit of the detector. The samples were purged with nitrogen for a minimum of 20 h in the humidity equilibrated samples, prior to exposure to an oxygen flow of 10 mL min^{-1}. A 5 cm^2 sample area was measured by using an in-house developed mask. The measurements were done in duplicate.

Mechanical Properties

Tensile tests were carried out at 24°C and 50% RH on an Instron 4400 Universal Tester. Pre-conditioned dumb-bell shaped specimens with initial gauge length of 25 mm and 5 mm in width were die-stamped from the films in the machine direction according to ASTM D638. The thickness of all specimens was approximately 100 μm. A fixed crosshead rate of 10 mm min^{-1} was used in all cases, and results were taken as the average of, at least, three tests.

Scanning Electron Microscopy (SEM)

For scanning electron microscopy (SEM) observation, the samples were cryofractured after immersion in liquid nitrogen, mounted on bevel sample holders and sputtered with Au/Pd under vacuum. The cross section images of the films were examined on a Hitachi microscope (Hitachi S-4100) at an accelerating voltage of 10 KV and a working distance of 12−16 mm.

Transmission Electron Microscopy (TEM)

Transmission electron microscopy (TEM) was performed using a JEOL 1010 (Jeol, Tokyo, Japan) equipped with a digital Bioscan (Gatan) image acquisition system. TEM observations were performed on ultrathin sections of microtomed thin composite sheets.

Statistical Analysis

Results were analyzed by multifactor analysis of variance (ANOVA) using Statgraphics Centurion 15.1 software (Statpoint Technologies, INC, Warrenton, VA). Tukey's test was used at the 95% confidence level.

RESULTS AND DISCUSSION

Morphology and Optical Properties of the PLA-BCNC Nanocomposites Obtained by Ball-Milling

The nanocomposite films obtained after compression moulding of the different formulations obtained through ball milling were optically identical to a neat PLA film (cf. Supporting Information Figure S1), which indicated that this processing method effectively broke up the aggregates formed during the freeze-drying of the BCNC. The development of PLA-BCNC films through the direct melt compounding of the biopolyester with the freeze-dried material is known to give rise to materials with aggregates that can be visually observed.[9,10]

The opacity values of the films with different BCNC content are shown in Table I. From this table it can be observed that only for the film with the greatest nanocellulose content there were significant differences in opacity, which increased with respect to the neat PLA film.

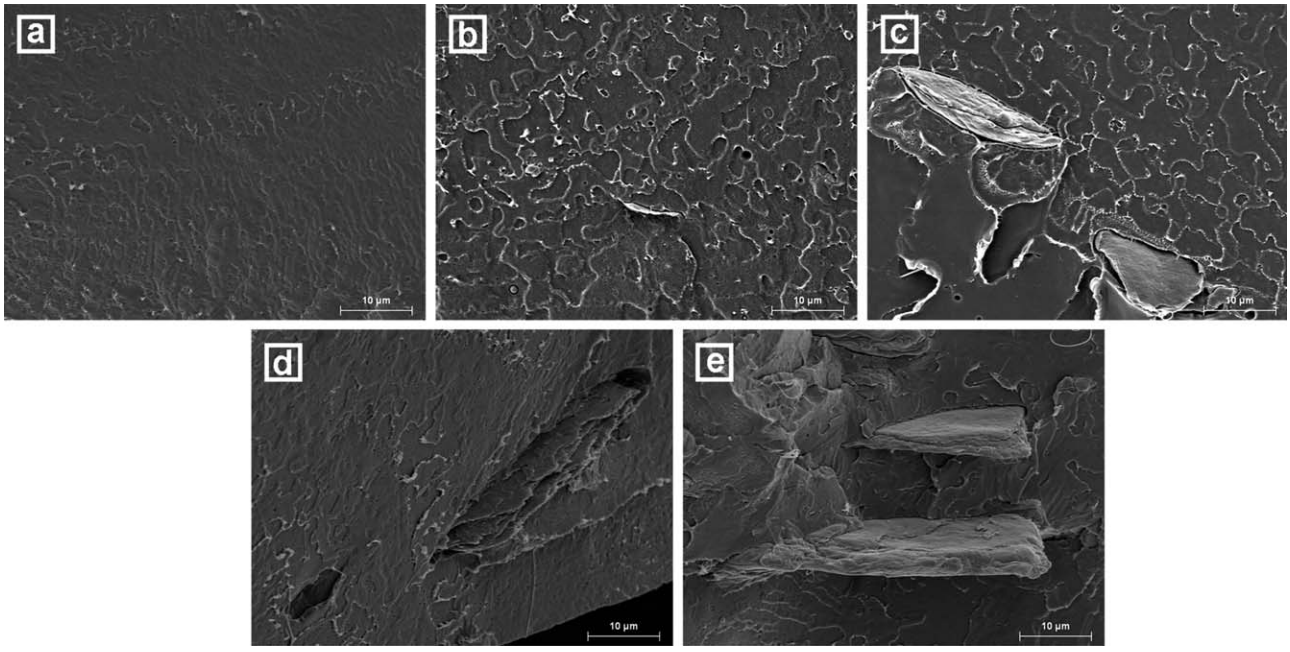

Figure 1. SEM images of the cross-sections of the different films obtained through ball-milling: (a) Neat PLA film; (b) PLA-BCNC 0.5%; (c) PLA-BCNC 1%; (d) PLA-BCNC 3%; (e) PLA-BCNC 5%. Scale markers correspond to 10 μm.

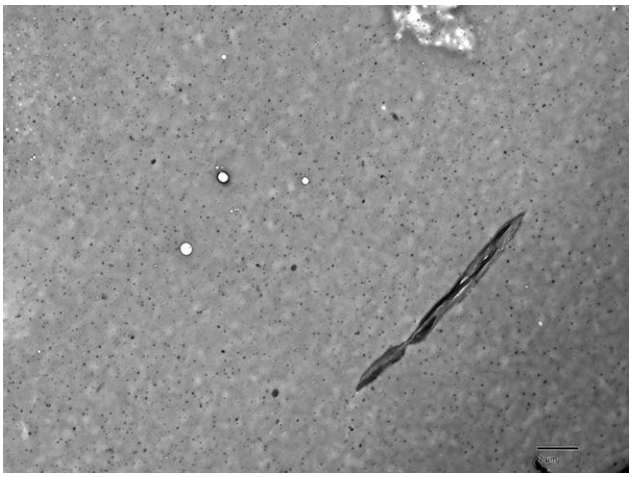

Figure 2. TEM micrograph of PLA-BCNC films containing 1 wt % BCNC. Scale markers correspond to 2 μm.

The microstructure of the films was also evaluated through SEM and TEM analysis. The cryo-fractured surfaces of the various nanocomposites in comparison with that of the neat PLA film are shown in Figure 1. From these images it can be observed that even though there were little optical differences at the macroscopic level, some nanocellulose aggregates still remain in the materials. Nevertheless, although these aggregates were also observed by TEM analysis, a significant fraction of the filler was properly dispersed and distributed as observed in Figure 2.

From the morphological study, it can be stated that although this technique broke up big aggregates so as to give rise to transparent films (in contrast with direct melt blending of PLA with freeze-dried BCNC), it was insufficient to attain a proper BCNC dispersion such as the one obtained using other pre-dispersion methods previously described.[9,10] Moreover, increasing the nanocellulose content in the materials resulted in bigger and more frequent aggregates as observed by SEM (cf. Figure 1).

Thermal Properties and Isothermal Crystallization

With the aim of investigating the effects of BCNC addition through the ball milling methodology on the thermal properties of the PLA nanocomposites, DSC analyses of all the samples were carried out. Table II compiles the melting temperature (T_m), melting enthalpy (ΔH_m) normalized to the PLA content of the nanocomposite films, and the cold crystallization temperature (T_{cc}) which were obtained from the DSC first heating run, and the glass transition temperature which was determined from both the first (T_{g1}) and the second heating run (T_{g2}). Furthermore, Figure 3 shows the thermograms from the first heating scan of each sample.

The first interesting observation was that the neat PLA film obtained after ball milling, showed a double melting event, suggesting the existence of two different crystalline populations, probably generated as a consequence of the mechanical treatment of the polymer. Several authors have reported that high energy ball milling applied to different polymers, such as poly(methyl methacrylate) (PMMA) and poly (lactic-co-glycolic acid) (PLGA), results in changes in the molecular weight of the polymers.[17,18] Specifically, chain scission has been observed in PMMA as a consequence of the intense mechanical treatment,[17] which could explain the development of lower melting temperature crystallites.

As deduced from the results in Table II, the thermal properties of the nanocomposites were not significantly different from those of the neat PLA film obtained through ball milling. Only a slight decrease in the cold crystallization temperature (T_{cc}) was observed for the nanocomposites. The lower T_{cc} observed in the heating run can be an indication of a faster crystallization induced by the presence of a significant fraction of well dispersed BCNC, as observed in TEM analysis, which acted as nucleating agents for PLA, as previously reported.[9,19] In fact, the crystallinity of the nanocomposites increased as a function of nanocellulose loading, supporting the beneficial effect of the fillers on crystallization. This is an interesting result, as it is well-known that, in general, ball milling of semicrystalline polymers results in decreased crystallinity.[20,21]

To further analyse the influence of BCNC on the crystallization process, an isothermal crystallization study was carried out. Three different crystallization temperatures were used (105, 110, and 115°C) for the study and Table III compiles the parameters obtained through fitting the DSC crystallization curves with the Avrami model [Equation (1)]:

$$X(t)=1-\exp\left(-kt^n\right) \quad (1)$$

where $X(t)$ is the relative crystallinity at time t, k is the crystallization rate constant, and n is the Avrami index. Derivative method reported by De Santis and Pantani[22] was used to

Table II. DSC Maximums of Melting (T_{m1} and T_{m2}), Melting Enthalpy (ΔH_m), Cold Crystallization Temperature (T_{cc}), Cold Crystallization Enthalpy (ΔH_c), PLA Crystallinity (X_c), and Glass Transition Temperature of PLA Films Processed by Ball Milling Obtained During the First (T_{g1}) and Second (T_{g2}) Heating Runs

	T_{m1} (°C)	T_{m2} (°C)	ΔH_m (J g^{-1})	T_{cc}	ΔH_c (J g^{-1})	X_c (%)	T_{g1}	T_{g2}
PLA	147.3	153.5	34.5	109.7	33.2	1.4	57.9	58.8
PLA-BCNC 0.5%	147.0	154.0	31.4	107.7	30.0	1.6	58.8	59.2
PLA-BCNC 1%	147.3	153.8	36.3	108.5	33.0	3.6	56.7	56.9
PLA-BCNC 3%	147.0	153.5	36.0	108.5	32.2	4.1	56.0	58.9
PLA-BCNC 5%	146.9	154.0	35.8	107.0	31.4	4.7	56.3	59.0

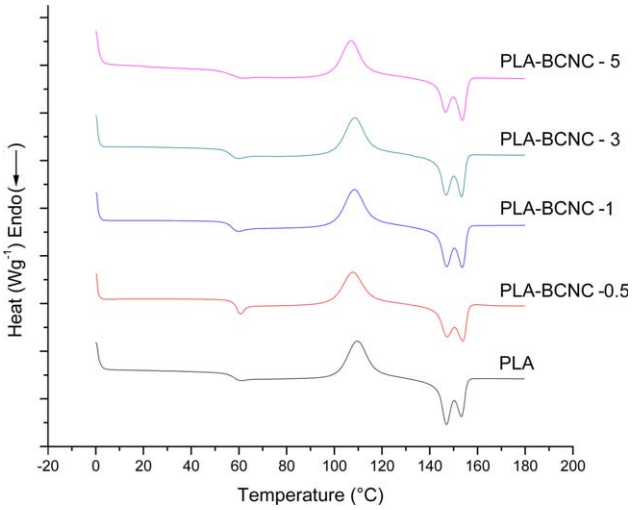

Figure 3. DSC first heating scan thermograms of PLA and its nanocomposites. [Color figure can be viewed in the online issue, which is available at wileyonlinelibrary.com.]

directly fit the calorimetric curve of the isothermal crystallization process to the derivative form of Avrami equation.

It is well-known that the value of the Avrami exponent n is related to the type of nucleation and to the geometry of the growing crystals, and usually is an integer between 1 and 4. At the different crystallization temperatures investigated, this exponent was in the vicinity of 3, both for the neat polymer and for the nanocomposites, thus suggesting that addition of the nanocellulose did not significantly affected the crystallization mechanism.

On the other hand, the parameter k has contributions from both nucleation and growth, and the increase in this parameter could be related with an increase in the crystallization rate and, thus, an improvement in the crystallization process. As shown in Table III, parameter k increased when increasing the BCNC content when the isothermal crystallization process was carried out at 110 and 115°C, thus pointing out to an acceleration of the crystallization process. In contrast, at 105°C, an increase in this parameter was only observed for PLA-BCNC 5% sample. At this temperature, that is, 105°C, the crystallization process went faster (as observed if comparing the k parameters at the three different temperatures) and, apparently, small additions of BCNC did not affect it. In contrast, the nanocomposite with 5 wt % BCNC content showed an acceleration of the crystallization process reflected in an increase of the parameter k. In line with these results, the crystallization half times ($t_{1/2}$, time required for half of the final crystallinity to develop) decreased for the nanocomposites when compared to the neat polymer at 110 and 115°C. At 105°C, since $t_{1/2}$ is directly related with the crystallization rate constant, the same trend was observed as for this parameter, no effect on the crystallization process for low contents of BCNC was observed, while the crystallization process was promoted when BCNC content was increased up to 5 wt %. The decrease of $t_{1/2}$ was also related to the nanofiller content, again indicating an increase in the crystallization rate promoted by the presence of nanocellulose. Increasing the crystallization temperature, the rate of nucleation decreased and thus the overall crystallization rate also decreased. Similar results were obtained during the isothermal cold crystallization of PLA using several nucleating agents,[23] thus confirming that BCNC effectively promoted crystallization acting as nucleating sites.

The thermal stability of the different materials obtained through ball milling and subsequently pressed into films were also analyzed using TGA in the presence of air and under a nitrogen atmosphere. In general, as observed in Table IV, incorporation of BCNC through the ball milling methodology did not alter the thermal stability of the nanocomposites. Despite the fact that native BCNC are less thermally stable than PLA,[7,9] no significant decrease in the thermal stability of the materials was observed and even a slight increase in the onset degradation temperature was noticed when the samples were analyzed in the presence of oxygen.

Mechanical and Thermo Mechanical Characterization

The mechanical properties of PLA and its corresponding BCNC-containing nanocomposite films obtained through ball milling are summarized in Table V. In general, the PLA films containing nanocellulose exhibited a higher Young's modulus and tensile strength and lower elongation at break than the neat PLA film, regardless of the nanofiller content. It is interesting to note that the greatest reinforcing effect observed corresponded to the film with lowest BCNC content (0.5%), probably as a consequence of the better dispersion of the nanofiller within the polymeric matrix, as inferred from the SEM micrographs. When comparing the ball milling methodology presented in this work with other strategies previously reported to develop PLA-BCNC nanocomposites,[9,10] the improvements in Young's modulus and tensile strength were lower than the previously reported ones, about a 10% improvement of both parameters using the ball

Table III. Parameters Obtained from the Avrami Analysis During Isothermal Crystallization of PLA and Its Nanocomposites Prepared by Ball Milling

	105°C			110°C			115°C		
	k (s^{-1})	n	$t_{1/2}$ (s)	k (s^{-1})	n	$t_{1/2}$ (s)	k (s^{-1})	n	$t_{1/2}$ (s)
PLA	1.2 e-3	3.2	734.3	8.0 e-4	3.0	1108.1	3.9 e-4	3.5	2281.4
PLA-BCNC 0.5%	1.1 e-3	3.2	845.7	8.4 e-4	3.1	1052.4	5.5 e-4	2.9	1606.2
PLA-BCNC 1%	1.1 e-3	3.4	836.4	8.5 e-4	2.9	1034.4	5.8 e-4	2.9	1531.0
PLA-BCNC 3%	1.0 e-3	3.3	851.8	9.3 e-4	3.0	956.8	8.6 e-4	2.8	1021.8
PLA-BCNC 5%	1.7 e-3	2.8	510.3	1.5 e-3	2.9	573.9	1.2 e-3	2.8	726.5

Table IV. TGA Maximum of the Weight Loss First Derivate (Td) and the Corresponding Peak Onset Values and the Residue at 600°C for the PLA Films, Analyzed in the Presence of Air (O_2) and Under a Nitrogen Atmosphere (N_2)

	Oxygen			Nitrogen		
	Onset T (°C)	Td (°C)	Residue at 600°C	Onset T (°C)	Td (°C)	Residue at 600°C
PLA	325.8	362.7	2.6	329.5	366.4	2.1
PLA-BCNC 0.5%	329.0	363.6	1.8	331.2	366.9	2.1
PLA-BCNC 1%	332.3	361.5	2.2	331.2	366.5	1.9
PLA-BCNC 3%	330.2	361.4	1.8	330.1	366.2	2.3
PLA-BCNC 5%	330.4	362.2	1.9	330.4	365.4	2.8

milling approach vs. 52 or 17% Young's modulus increase and 31 or 14% tensile strength increase for BCNC incorporation through grafting with lactic acid oligomers[10] or pre-incorporation through electrospinning,[9] respectively. Chemical grafting of BCNC with poly(glycidyl methacrylate) (PGMA) before incorporation into PLA also resulted in slightly better mechanical properties, reaching improvements of ca. 16 and 22% in Young's modulus and tensile strength, respectively.[11]

The load bearing capacity of neat PLA and BCNC-containing nanocomposites obtained through ball milling was studied from the storage modulus. The results are shown in Figure 4(a). The storage modulus of the PLA nanocomposite films improved over the entire temperature span as compared to neat PLA. The increase in the storage modulus was directly related to the nanofiller content and could be attributed, not only to the presence of the nanofiller, but also to the observed increase in crystallinity of the nanocomposites (cf. Table II).

The ratio of loss modulus to storage modulus is defined as mechanical loss factor or tan delta. Figure 4(b) shows that incorporation of the BCNC led to an increase of about 3°C in the tan delta peak of PLA. These increments were attributed to the restricted segmental mobility of the matrix chains around the nanofillers.[24] However, the increase was not proportional to the nanofiller content, probably due to agglomeration and; thus, increasing the BCNC amount did not correlate with increased surface area for interaction with the biopolyester.

Barrier Properties

Finally, the oxygen permeability of the nanocomposites obtained through ball milling in comparison with the neat PLA film was also characterized at 80% RH. The results are plotted in Figure 5.

The oxygen permeability of neat PLA obtained through ball milling was very similar to that previously reported in the literature,[25,26] even though that, as previously stated, ball milling processing leads to an increase in density of the material.[27]

From Figure 5 it can be observed that a significant reduction in the oxygen permeability was obtained for the materials containing BCNC, suggesting that the well dispersed fraction of crystalline nanofillers effectively blocked the oxygen flow, although the greatest reduction was seen for the lowest nanocellulose content, highlighting again the importance of dispersion to optimize the performance improvements in this kind of films. When comparing the results of this study with previous PLA-BCNC nanocomposites prepared using different routes and methodologies, it can be stated that ball milling improved the dispersion of the nanofillers when compared to PGMA-grafted BCNC nanocomposites[11] or direct freeze-dried nanocellulose addition, which led to a lower improvements or deleterious effect on barrier properties, respectively. However, greater improvements were obtained using pre-incorporation methods such as dispersion in electrospun fibres[9] or grafting with lactic acid oligomers,[10] which improved the further dispersion in PLA matrix through melt compounding. Moreover, in a comparision with PLA-based nanocompounds reinforced with nanoclays,[28,29] lower improvements were obtained in this study. It is important to mention that, in one hand, the used methodology to incorporate the nanofiller were different to that used in this study. In fact, to the best of our knowledge, there is no any literature about the incorporation of nanoclays into PLA through ball milling. On the other hand, the better improvements obtained in those studies were due to the filler nature. It is widely known that its lamellar structure induced higher blocking effect to the vapor and gases pathways.

Table V. Young's Modulus (E), Tensile Strength, and Elongation at Break (ε_b) for PLA and its Nanocomposites with BCNC Obtained Through Ball Milling

	E (MPa)	Tensile strength (MPa)	ε_b (%)
PLA	2091.9 ± 190.6	41.36 ± 4.5	4.8 ± 2.0
PLA-BCNC 0.5%	2305.4 ± 96.0	45.40 ± 2.4	3.4 ± 0.4
PLA-BCNC 1%	2120.7 ± 136.6	42.67 ± 2.5	3.4 ± 0.5
PLA-BCNC 3%	1953.6 ± 125.9	38.83 ± 3.9	2.6 ± 0.4
PLA-BCNC 5%	2176.2 ± 56.6	40.24 ± 4.3	2.4 ± 0.4

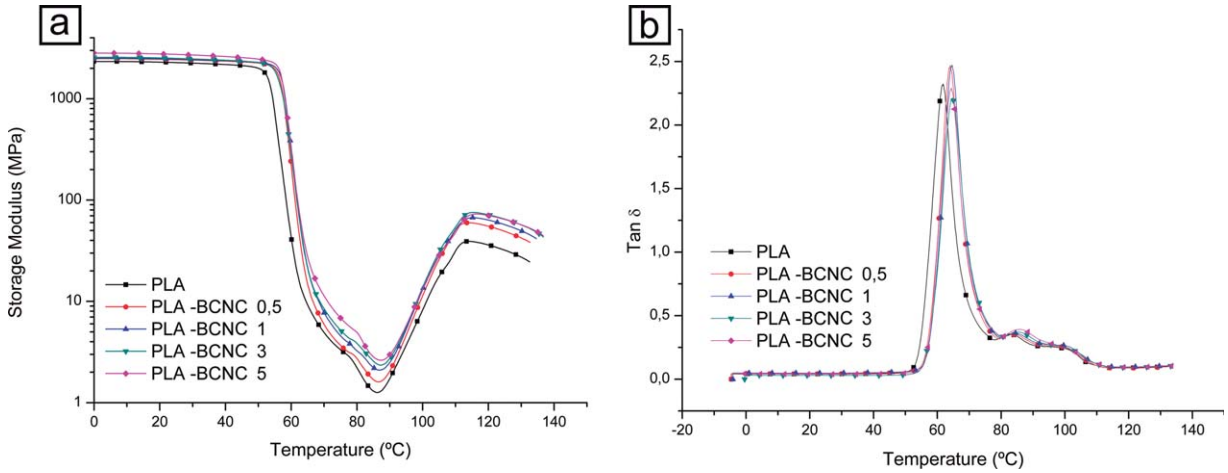

Figure 4. Storage modulus (a) and tan delta (b) plots versus temperature for neat PLA and its nanocomposites films with BCNC. [Color figure can be viewed in the online issue, which is available at wileyonlinelibrary.com.]

CONCLUSIONS

In this work it has been demonstrated that ball milling can lead to a significant dispersion of the BCNC filler within a PLA matrix when compared to direct addition of freeze-dried nanocellulose in a melt mixing process. The morphological studies showed that this technique was able to disperse and distribute the freeze dried BCNC fillers, although some agglomerates remained. Upon increasing the BCNC content an increase in the number of aggregates were observed. The well dispersed fraction of BCNC acted as nucleating sites, increasing the crystallization rate and the final crystallinity index of the materials. Moreover, thermal stability was not significantly affected and even a slight increase in the onset degradation temperature was observed in the nanocomposites obtained through ball milling. Improved thermo-mechanical and barrier properties were observed for nanocomposites as compared to the neat PLA. In spite of this, the nanocomposite film with lowest BCNC content displayed the best performance in terms of mechanical and thermo-mechanical properties, as well as permeability to oxygen measured at high relative humidity, which was related to a better dispersion of the nanofiller at this loading level.

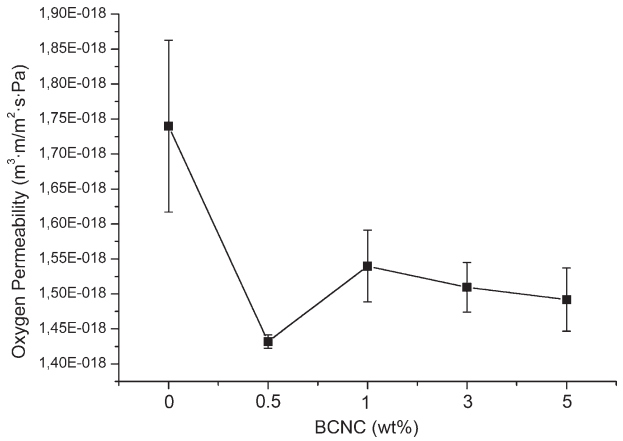

Figure 5. Oxygen permeability measured at 80% RH for neat PLA and its nanocomposites with BCNC prepared by ball milling.

ACKNOWLEDGMENTS

J. Ambrosio-Martín would like to thank the Spanish Ministry of Economy and Competitiveness for the FPI grant BES-2010-038203. M.J. Fabra is recipient of a "Juan de la Cierva" contracts from the Spanish Ministry of Economy and Competitiveness. The authors acknowledge financial support from the MINECO (MAT2012-38947-C02-01 project).

REFERENCES

1. Araki, J.; Wada, M.; Kuga, S.; Okano, T. *Colloids Surf. A* **1998**, *142*, 75.
2. Favier, V.; Chanzy, H.; Cavaille, J. Y. *Macromolecules* **1995**, *28*, 6365.
3. Siqueira, G.; Bras, J.; Dufresne, A. *Biomacromolecules* **2009**, *10*, 425.
4. Araki, J.; Kuga, S. *Langmuir* **2001**, *17*, 4493.
5. De Souza Lima, M. M.; Wong, J. T.; Paillet, M.; Borsali, R.; Pecora, R. *Langmuir* **2003**, *19*, 24.
6. Hirai, A.; Inui, O.; Horii, F.; Tsuji, M. *Langmuir* **2009**, *25*, 497.
7. Martínez-Sanz, M.; Lopez-Rubio, A.; Lagaron, J. M. *Carbohydr. Polym.* **2011**, *85*, 228.
8. Lunt, J. *Polym. Degrad. Stab.* **1998**, *59*, 145.
9. Martínez-Sanz, M.; Lopez-Rubio, A.; Lagaron, J. M. *Biomacromolecules* **2012**, *13*, 3887.
10. Ambrosio-Martín, J.; Fabra, M. J.; Lopez-Rubio, A.; Lagaron, J. M. *Cellulose* **2014**, Unpublished.
11. Martínez-Sanz, M.; Abdelwahab, M. A.; Lopez-Rubio, A.; Lagaron, J. M.; Chiellini, E.; Williams, T. G.; Wood, D. F.; Orts, W. J.; Imam, S. H. *Eur. Polym. J.* **2013**, *49*, 2062.
12. Perrin-Sarazin, F.; Sepehr, M.; Bouaricha, S.; Denault, J. *Polym. Eng. Sci.* **2009**, *49*, 651.
13. Wu, H.; Zhao, W.; Chen, G. *J. Appl. Polym. Sci.* **2012**, *125*, 3899.
14. Baheti, V.; Militky, J.; Marsalkova, M. *Polym. Compos.* **2013**, *34*, 2133.
15. Martínez-Sanz, M.; Olsson, R. T.; Lopez-Rubio, A.; Lagaron, J. M. *Cellulose* **2011**, *18*, 335.

16. Sanchez-Garcia, M. D.; Lagaron, J. M. *Cellulose* **2010**, *17*, 987.
17. Pantaleón, R.; González-Benito, J. *Polym. Compos.* **2010**, *31*, 1585.
18. Shabir, A.; Alhusban, F.; Perrie, Y.; Mohammed, A. R. *J. Basic Clin. Pharm.* **2011**, *2*, 71.
19. Suryanegara, L.; Nakagaito, A. N.; Yano, H. *Cellulose* **2010**, *17*, 771.
20. Ishida, T. *J. Mater. Sci. Lett.* **1994**, *13*, 623.
21. Olmos, D.; Domínguez, C.; Castrillo, P. D.; Gonzalez-Benito, J. *Polymer* **2009**, *50*, 1732.
22. De Santis, F.; Pantani, R. *J. Therm. Anal. Calorim.* **2013**, *112*, 1481.
23. Liao, R.; Yang, B.; Yu, W.; Zhou, C. *J. Appl. Polym. Sci.* **2007**, *104*, 310.
24. Avérous, L.; Fringant, C.; Moro, L. *Polymer* **2001**, *42*, 6565.
25. Petersen, K.; Nielsen, P. V.; Olsen, M. B. *Starch/Staerke* **2001**, *53*, 356.
26. Sanchez-Garcia, M. D.; Nordqvist, D.; Hedenqvist, M.; Lagaron, J. M. *J. Appl. Polym. Sci.* **2011**, *119*, 3708.
27. Takamatsu, H.; Miyazaki, T.; Ishida, E.; Ashizuka, M.; Abe, H. *J. Ceram. Soc. Jpn.* **2006**, *114*, 332.
28. Tenn, N.; Follain, N.; Soulestin, J.; Crétois, R.; Bourbigot, S.; Marais, S. *J. Phys. Chem. C* **2013**, *117*, 12117.
29. Sanchez-Garcia, M. D.; Lopez-Rubio, A.; Lagaron, J. M. *Trends. Food. Sci. Tech.* **2010**, *21*, 528.